© 2016. Published by The Company of Biologists Ltd | Journal of Experimental Biology (2016) 219, 3028-3038 doi:10.1242/jeb.141234

RESEARCH ARTICLE

Voltage-gated calcium channels of *Paramecium* cilia

Sukanya Lodh*, Junji Yano*,‡, Megan S. Valentine and Judith L. Van Houten

ABSTRACT

Paramecium cells swim by beating their cilia, and make turns by transiently reversing their power stroke. Reversal is caused by Ca^{2+} entering the cilium through voltage-gated Ca^{2+} (Ca_V) channels that are found exclusively in the cilia. As ciliary Ca^{2+} levels return to normal, the cell pivots and swims forward in a new direction. Thus, the activation of the Ca_V channels causes cells to make a turn in their swimming paths. For 45 years, the physiological characteristics of the *Paramecium* ciliary Ca_V channels have been known, but the proteins were not identified until recently, when the *P. tetraurelia* ciliary membrane proteome was determined. Three $Ca_V\alpha1$ subunits that were identified among the proteins were cloned and confirmed to be expressed in the cilia. We demonstrate using RNA interference that these channels function as the ciliary Ca_V channels that are responsible for the reversal of ciliary beating. Furthermore, we show that Pawn (*pw*) mutants of *Paramecium* that cannot swim backward for lack of Ca_V channel activity do not express any of the three Ca_V1 channels in their ciliary membrane, until they are rescued from the mutant phenotype by expression of the wild-type *PW* gene. These results reinforce the correlation of the three Ca_V channels with backward swimming through ciliary reversal. The PwB protein, found in endoplasmic reticulum fractions, co-immunoprecipitates with the Ca_V1c channel and perhaps functions in trafficking. The PwA protein does not appear to have an interaction with the channel proteins but affects their appearance in the cilia.

KEY WORDS: *Paramecium*, Cilia, Voltage-gated calcium channel, $Ca_V\alpha1$, Pawn genes, Trafficking

INTRODUCTION

Cilia are slender organelles that protrude from eukaryotic cell surfaces. Depending on the cell type, there may be a solitary primary cilium or multiple cilia on a cell surface. These cilia have in common internal microtubule structures called axonemes, and those cilia with additional motor protein machinery in their axoneme can be motile. Primary cilia generally are immotile. The cilia of multi-ciliated cells usually are motile and contribute to the flow of spinal fluid or mucous in the airways. When cilia are dysfunctional, they contribute to a class of diseases called ciliopathies that are complex syndromes of developmental abnormalities. Regardless of superficial differences, all cilia are antennae for eukaryotic cells to sense many kinds of environmental stimuli (Berbari et al., 2009; Bloodgood, 2010; Brenker et al., 2012; Pazour and Witman, 2003; Singla and Reiter, 2006; Valentine et al., 2012).

Department of Biology, University of Vermont, Burlington, VT 05405, USA.
*These authors contributed equally to this work

‡Author for correspondence (Junji.Yano@uvm.edu)

J.Y., 0000-0001-6600-3624

Received 31 March 2016; Accepted 19 July 2016

As antennae, cilia detect stimuli such as odorants or mechanical forces, and convert these stimuli to intra-ciliary signals (reviewed in Bloodgood, 2010; Kleene and Van Houten, 2014; Lishko and Kirichok, 2015). Although the identities of channels and the roles of ciliary versus cellular sources of Ca^{2+} are now under re-examination for mammalian primary and ependymal and nodal cilia (DeCaen et al., 2013; Delling et al., 2013, 2016; Blum and Vick, 2015; Lee et al., 2015; Doerner et al., 2015), for protists and sperm, the influx of Ca^{2+} into cilia is clearly through the ciliary voltage-gated Ca^{2+} (Ca_V) channels in response to chemical signals, mechanosensation or depolarization. Calcium levels in the cilia control signaling output, such as the beat form and force of motile cilia or cell proliferation (Bloodgood, 2010; Kleene and Van Houten, 2014).

Whether cilia are solitary or numerous, motile or non-motile, ion channels control the intra-ciliary calcium levels, which play important roles in sensory transduction (Bloodgood, 2010). For example, cyclic nucleotide-gated Ca^{2+} channels that are found only in the immotile cilia of olfactory neurons open as part of the signal transduction pathway initiated by odorant binding to its receptor (Pifferi et al., 2006; Kleene, 2008). Motile cilia similarly have ion channels that participate in sensory transduction. For example, the Ca_V channel of the *Chlamydomonas* flagellum is necessary for the change in waveform in response to light or mechanical stimulation (Fujiu et al., 2011, 2009). The TRP family member polycystin-2 (PKD2) in *Chlamydomonas* flagella is crucial for the mating process that is dependent upon a Ca^{2+} influx (Huang et al., 2007). The CatSper Ca^{2+} channels of the sperm flagellum are responsible for the change in waveform in the vicinity of the egg (Brenker et al., 2012).

Because cilia are so highly conserved, it is possible to use a model system such as the ciliate *Paramecium tetraurelia* to provide insights into the ciliary calcium compartment and ciliary ion channel function. *Paramecium tetraurelia*, which is a cell covered in cilia, responds to sensory stimuli with changes in swimming behavior that result from changes in ciliary beating (Kung and Saimi, 1982; Machemer, 1988). Ciliary beat frequency and form are controlled by intra-ciliary Ca^{2+}, which, in turn, is controlled by action potentials of Ca_V channels. The Ca_V channels, which are necessary for the action potential and increase in intra-ciliary calcium, are found exclusively in the cilia (Dunlap, 1977). Depolarizing stimuli, such as mechanical stimulation and high K concentrations, activate this channel and initiate the calcium action potential. The Ca^{2+} entering the cilium through the Ca_V channels affects the ciliary beating, reversing the power stroke and transiently sending the cell swimming backward. As ciliary Ca^{2+} levels return to normal, the cell pivots in place and then swims forward in a new direction. Thus, the activation of the voltage-gated calcium current [$I_{Ca(V)}$] of the Ca_V channels causes cells to swim backward transiently and make a turn in their swimming paths (Eckert, 1972; Machemer, 1988).

For almost 50 years, the physiological characteristics of the *Paramecium* ciliary Ca_V channels have been known (reviewed in Eckert, 1972; Machemer, 1988), but the proteins were not identified until recently, when the *P. tetraurelia* ciliary membrane proteome

Journal of Experimental Biology

Journal of Experimental Biology (2016) 219, 3028-3038 doi:10.1242/jeb.141234

List of symbols and abbreviations

BSA	bovine serum albumin
Ca_V	voltage-gated Ca^{2+} (channel)
ER	endoplasmic reticulum
$I_{Ca(v)}$	voltage-gated calcium current
ID	immunodevelopment
IP	immunoprecipitation
MS	mass spectrometry
PMCA	plasma membrane calcium ATPase
pw	Pawn
RNAi	RNA interference
WGD	whole genome duplication

was determined. The three $Ca_V\alpha1$ subunits that were identified among the proteins (Yano et al., 2013) were subsequently cloned and confirmed to be expressed in the cilia (Valentine et al., 2012; present study). Here we demonstrate using RNA interference (RNAi) that these channels function as the ciliary Ca_V channels that are responsible for the reversal of ciliary beating. Furthermore, we have turned to the important mutants of *Paramecium* called Pawns (*pw*), which are named for the chess piece because they cannot swim backward for lack of ciliary Ca_V channel activity (Satow and Kung, 1974). Here we show that *pw* mutants do not express the Ca_V1a, b or c channels in their ciliary membrane. However, when the *pw* mutants are rescued from the mutant phenotype (i.e. swim backward and turn) by expression of the wild-type *PW* gene, the Ca_V1a, b and c channels can be found in the ciliary membrane as in the wild type, reinforcing the correlation of these three Ca_V channels with the calcium action potential that causes backward swimming through ciliary reversal.

MATERIALS AND METHODS

Stock and cultures

Paramecium tetraurelia wild-type (51s sensitive to killer), *nd6* (non-trichocyst discharge mutant, courtesy of Dr Jean Cohen, Centre de Génétique Moléculaire, Gif-sur-Yvette, France), *pwA* (d4-94), *pwA-nd6* double mutant (d4-94-nd6) and *pwB* (d4-95) cells were used. The cells were cultured in wheat grass infusion medium inoculated with *Aerobactor aerogenes* (Sasner and Van Houten, 1989; Wright and Van Houten, 1990).

Sequence analysis

Previous physiological studies indicated that the Ca_V channels of the action potential were exclusively in the cilia (Dunlap, 1977; Machemer and Ogura, 1979), which led our search for Ca_V channels to the cilia. We describe three putative Ca_V α1 subunit genes as identified in our proteomic study of *P. tetraurelia* ciliary membrane: GSPATG00010323001 *Ca_V1a*, GSPATG00033414001 combined with GSPARG00033415001 *Ca_V1b*, and GSPATG00017333001 *Ca_V1c* (Yano et al., 2013) (see Fig. 1, Table S1). The genes for *Ca_V1a* and *b* are paralogs and are closely related to the gene for *Ca_V1c*.

We used OMIGA 2.0 and DS GENE (Accelrys, San Diego, CA, USA) for multiple alignments of the *P. tetraurelia* sequences with the primary structures of Ca_V α-subunits from all three mammalian subfamilies (*Ca_V1–3*) (McRory et al., 2001; Mikami et al., 1989; Starr et al., 1991; Tyson and Snutch, 2013). We analyzed the sequences of the *Ca_V1a–c* genes for expected conserved domains (Fig. 1). We used TMHMM Server v. 2.0 (http://www.cbs.dtu.dk/services/TMHMM/) and SOSUI (http://bp.nuap.nagoya-u.ac.jp/sosui/sosuimenu0.html) for domain analysis. Calmodulin Target Database (http://calcium.uhnres.utoronto.ca/ctdb/ctdb/sequence.html) was used to locate putative calmodulin binding domains.

Feeding RNAi

Segments of 2055, 1688 and 1514 bp corresponding to the sequences between putative domains II and IV in *Ca_V1a*, *1b* and *1c* genes, respectively, were amplified by PCR using genomic macronuclear DNA as template (Yano et al., 2003) (for a diagram of these channels, see Fig. 1). PCR primers for this process are shown in Table S2. The 23-mers that could theoretically be generated by RNAi were compared with other genes using the RNAi off-target tool in ParameciumDB (http://paramecium.cgm.cnrs-gif.fr/cgi/tool/alignment/off_target.cgi). Any off-target overlap from the RNAi constructs and other channels is shown in Table S3.

The PCR products were ligated to the vector L4440 (AddGene, Cambridge, MA, USA), using restriction enzymes (Xho1 and Xba1, New England BioLabs, Ipswich, MA, USA) and a ligation kit (Ligate IT, Affymetrix, Santa Clara, CA, USA). The plasmid (empty or with insert) was transformed into strain HT115 of *Escherichia coli* following the manufacturer's instructions. The feeding RNAi experiments were performed following a published protocol (Valentine et al., 2012).

Backward swimming assay

All solutions for testing swimming behavior contain a base buffer of 1 mmol l^{-1} Tris and 1 mmol l^{-1} calcium citrate. 100 mmol l^{-1} Tris was used to adjust the pH of solutions to pH 7.0. Cells from the control and test RNAi cultures were transferred to depression slides with a resting solution, 4 mmol l^{-1} KCl in base buffer, pH 7.0, for 20 min. Cells were then transferred one by one to depressions with the test solution (30 mmol l^{-1} KCl in base buffer, pH 7.0). The control cells first whirled or jerked and then swam backward. At the end, they whirled again and started swimming forward. The durations of backward swimming, measured using a stopwatch, were analyzed using Mann–Whitney *U*-tests. We also used 8 mmol l^{-1} $BaCl_2$ in base buffer, pH 7.0, as the depolarization solution to induce backward swimming in *pw* mutants that were injected with wild-type sequences of the *PWA* or *PWB* genes.

Expressing tagged proteins from plasmids

The wild-type *PWA* (AF050753) and *PWB* (AF179276) genes were amplified by PCR using macronuclear genomic DNA. The primers used for amplification and restriction enzymes used for cloning into the expression plasmids are shown in Table S4. The PCR products were ligated into the vector pPXV (Haynes et al., 1995), or into pPXV with 3×Myc or 3×FLAG sequences for C-terminus tagging of the expressed protein (Valentine et al., 2012). Full-length sequences from the Ca_V channels *Ca_V1a* and *1b* were amplified by PCR using TaKaRa LA *Taq* DNA polymerase (Takara/Clontech, Mountain View, CA, USA) and inserted into the pPXV with a 3×FLAG tag at the N terminus following our previously published description of inserting *Ca_V1c* into pPXV-3×FLAG for an N-terminal tag (Valentine et al., 2012; Yano et al., 2013). Inserted sequences were confirmed by the DNA sequencing in the Vermont Cancer Center Advanced Genome Technologies Core.

Microinjection of expression plasmid

Following established procedures (Haynes et al., 1995; Yano et al., 2013), a solution of linearized plasmid (5 µg $µl^{-1}$) was injected into the macronuclei of cells; the individual injected cells were cultured. The plasmid with the *PWA* or tagged *PWA* or *PWB* sequence was

Journal of Experimental Biology (2016) 219, 3028-3038 doi:10.1242/jeb.141234

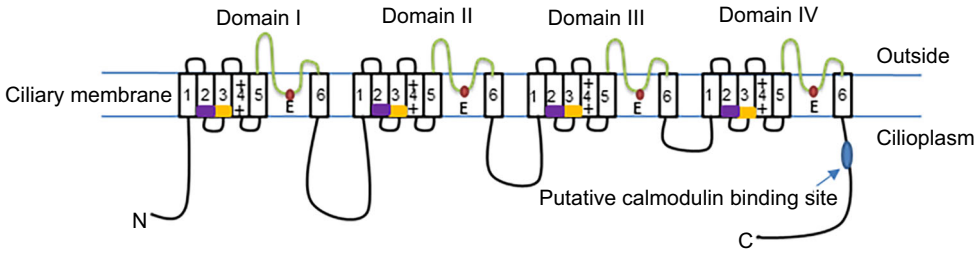

Fig. 1. Primary structure of $Ca_V\alpha1$ subunit in *Paramecium tetraurelia*. The Ca_V1c protein is predicted to have four homologous domains (domains I–IV). Each domain consists of six transmembrane segments (s1–6). The fourth segment in each domain works as a voltage sensor. The voltage sensor consists of four conserved positively charged residues (+4+) at every third residue in s4. The four pore loops (light green) between the fifth and sixth segments from each domain form a selective filter through which divalent cations can pass (Mikami et al., 1989; Starr et al., 1991; McRory et al., 2001). In the mammalian Ca_V1 and 2 subfamilies, the consensus sequence found in each of the four pore loops that forms the filter site for divalent cation selection is TxExW. The four glutamic acid residues (E) are thought to be the site for the binding and selection of the divalent cation. In *P. tetraurelia* Ca_V1c, all four pore loops have an E (red oval). Two other conserved sites, FxxExxxK located in s2 and NxxD located in s3, are shown as purple and orange boxes, respectively. When we analyzed the Ca_V1c protein for a putative calmodulin binding site, we located one in the C-terminal cytoplasmic tail (blue oval). Among the cytoplasmic loops, the loop between domains I and II is the longest, estimated to be 684 amino acids. The Ca_V1c paralogs Ca_V1a and 1b have the same predicted structure.

injected into the macronucleus of *pwA-nd6* or *pwA* (d4-94) cells, and the plasmid with *PWB* or tagged *PWB* into the macronucleus of *pwB* (d4-95) cells. When *FLAG-Ca$_V$1*s and *PWA* wild-type or *PWB* wild-type genes (with or without tags) were to be co-expressed, the *FLAG-Ca$_V$1* plasmids were the first plasmids injected into wild-type or *pw* mutant cells.

Genomic DNA from the cell lines was used as template in PCR to determine which lines had the highest concentration of exogenous gene copies for a second injection of a different plasmid or further experiments. To do so, the endogenous and exogenous (plasmid) DNAs were separately amplified by PCR, using a forward primer from the coding region, and a reverse primer from its 3′ untranscribed region (for endogenous sequences) or calmodulin 3′ untranscribed region of pPXV plasmid (for exogenous plasmid sequences). The intensity of PCR bands from endogenous and exogenous mRNA were analyzed using ImageJ (National Institutes of Health, Bethesda, MD, USA) to compare indirectly the relative amounts of plasmid copies in cell lines. Cells injected with plasmids containing the epitope tag sequence only were used as a control to match the experimental cells in each experiment.

Whole-cell lysates

Two to three milliliters of packed cells were collected from 3 to 6 liters of control and test cultured cells. The cells were washed twice in Dryl's solution (1 mmol l^{-1} Na_2HPO_4, 1 mmol l^{-1} NaH_2PO_4, 2 mmol l^{-1} trisodium citrate, 1.5 mmol l^{-1} $CaCl_2$) and once in cold LAP200 (50 mmol l^{-1} HEPES, pH 7.4, 200 mmol l^{-1} KCl, 1 mmol l^{-1}, EGTA, 1 mmol l^{-1} $MgCl_2$) with protease inhibitors [1 mmol l^{-1} phenylmethylsulfonyl fluoride (PMSF, Sigma-Aldrich, St Louis, MO, USA), 0.1 µg ml^{-1} Pepstatin (Research Products International, Mt Prospect, IL, USA), 0.1 µg ml^{-1} Leupeptin (Research Products International) and protease inhibitor cocktail (Sigma-Aldrich) at a final concentration of 0.1%]. The washed cells were resuspended in 5 ml of LAP200 buffer with the protease inhibitors and maintained at 4°C while being homogenized until 95% of the cells were ruptured.

Pellicles and subcellular P2 and P10 pellets

For work flow, see Fig. 2. The pellicles (cell surface membranes with cytoskeleton) were prepared as described previously (Wright and Van Houten, 1990). In this preparation, cells were washed three times in cold HM buffer (20 mmol l^{-1} maleic acid, 20 mmol l^{-1} Tris, 1 mmol l^{-1} Na_2EDTA, pH 7.8) instead of Dryl's solution. The cells were homogenized in HM buffer with the protease inhibitors at 4°C. The pellet was washed, collected as the 'pellicle' and further treated with detergent and centrifugation to produce a supernatant for immunoprecipitation (IP). The first supernatant from the pellicle preparation was vortexed vigorously for 5 min and centrifuged at 2000 ***g*** for 10 min at 4°C. The supernatant was then centrifuged at 19,800 ***g*** for 30 min at 4°C to produce the pellet P2. The resulting supernatant was centrifuged at 100,000 ***g*** for 1 h at 4°C to produce the pellet P10. Intracellular membranes with an enzyme signature (glucose-6-phosphatase) of the endoplasmic reticulum (ER) are reported to be enriched in the P2 and P10 pellets (Haga et al., 1984; Wright and Van Houten, 1990; S. Lodh, Characterization of PWA and PWB proteins in *Paramecium*, PhD dissertation, University of Vermont, 2012). The pellicle, P2 or P10, were resuspended in membrane buffer (10 mmol l^{-1} Tris buffer, pH 7.4, 50 mmol l^{-1} KCl, 5 mmol l^{-1} $MgCl_2$, 1 mmol l^{-1} EGTA) or LAP200 buffer with the protease inhibitors (1 mmol l^{-1} PMSF, 0.1 µg ml^{-1} Pepstatin, 0.1 µg ml^{-1} Leupeptin and 0.1% protease inhibitor cocktail) at 4°C (Haga et al., 1982, 1984; Wright and Van Houten, 1990).

Cytoplasmic factors that cure the three *pw* mutants and restore action potentials and backward swimming are thought to be in the subcellular membrane fraction; the fraction that we refer to as P10 is the equivalent of the 'P2' fraction that Haga and others used to cure *P. tetraurelia pw* mutants by injection (Haga et al., 1982, 1984).

Cilia isolation

The cilia from the control and test cells were isolated from 2–3 ml of packed cells collected from 3–6 liters of cell culture following the protocol of Yano and co-workers (Yano et al., 2013). The isolated cilia were suspended in 1 ml of membrane buffer or LAP200 with protease inhibitor at the same concentration previously described at 4°C.

Protein assay

The protein concentration of each sample was measured using the Pierce Protein Assay (Thermo Fisher Scientific, Waltham, MA, USA). The cilia samples from the control and test were adjusted to the same volume and protein concentration for further experiments.

Immunoprecipitation (IP)

Triton X-114 for solubilizing Ca_V1s, calcium ATPases (PMCA) or Pw proteins, or Triton X-100 for solubilizing Pw proteins (as

Journal of Experimental Biology (2016) 219, 3028-3038 doi:10.1242/jeb.141234

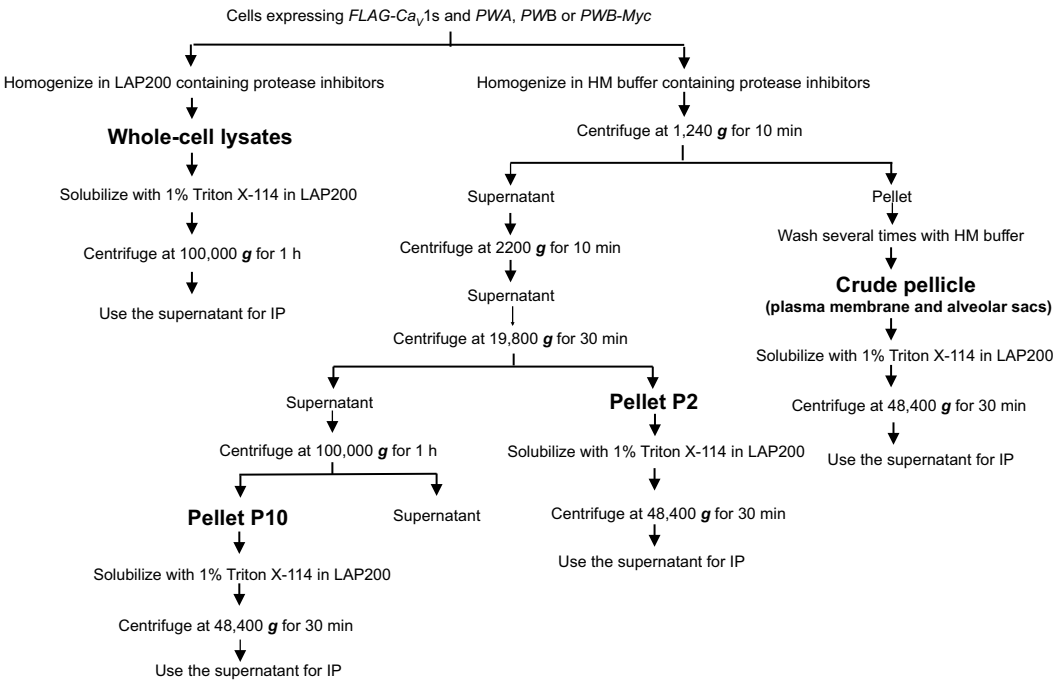

Fig. 2. Protocol for subcellular fractionation (P2 and P10) and crude pellicle and whole-cell lysate preparation.

indicated in each specific figure) was added to the whole-cell lysate, pellicle, P2, P10 or cilia suspension to achieve a final concentration of 1%. Each sample was agitated by rocking at 4°C for 1 h followed by centrifugation at 48,400 ***g*** (pellicle and cilia) or 100,000 ***g*** (whole-cell lysate and P10) at 4°C for 30 min. The supernatant was incubated with 20 µl Protein A beads (Amersham Pharmacia/GE HealthCare, Pittsburgh, PA, USA) at 4°C for 1 h to clarify the supernatant. Prior to use, the Protein A beads had been washed in membrane buffer or LAP200 buffer with 1% Triton and 1% (w/v) bovine serum albumin (BSA). After removing the beads by centrifugation at 48,400 ***g*** at 4°C for 30 min, the clarified supernatant was incubated with 20 µl of anti-FLAG M2 affinity agarose (Sigma-Aldrich), or anti-c-Myc (polyclonal antibody) affinity agarose (Sigma-Aldrich) at 4°C for 1 h, which had been pre-washed in the membrane buffer or LAP200 with 1% Triton and 1% BSA.

Next, the antibody-conjugated beads were washed three times by centrifugation at 8000 ***g*** in the membrane buffer or LAP200 with 1% Triton and 1% BSA and three times in the buffer without Triton and BSA. The beads were suspended in 50 µl of 2× sodium dodecyl sulfate (SDS) buffer (6.25 mmol l^{-1} Tris, 1.5% SDS, 1% glycerol, 0.001% Bromophenol Blue, pH 6.8) with or without 3% β-mercaptoethanol, and boiled for 10 min. After centrifuging at 14,000 ***g*** at 4°C, the supernatant was loaded onto a 4–18% or 7–18% gradient SDS-polyacrylamide gel (SDS-PAG) and run at the constant current of 20 mA. To confirm that approximately the same amounts of protein went into the control and test IPs, we removed 20 µl of the test and control samples, clarified the Triton-treated supernatants and analyzed the proteins on western blots using α-tubulin as a protein that should not vary between control and test samples.

For the IP of the Ca_V channels from the ciliary membrane, plasma membrane calcium ATPases (PMCAs) were used to assess gel loading. The same IP protocol as described above for cells expressing *FLAG-Ca$_V$1c* was used. In addition, the supernatant that had been clarified with Protein A beads was incubated with 5 µg of rabbit anti-calmodulin binding domain antibody of *P. tetraurelia* PMCA2 (anti-CBD2 antibody) (Van Houten, 1998) at 4°C for 1 h followed by the incubation with Protein A beads for IP.

Western blot analysis

We examined the subcellular localization of expressed epitope-tagged PwA and PwB proteins by western blot analysis. A total of 100 µg of protein from the pellicle, P2, P10, or cilia suspension that was prepared from both the test and control cells were run on 12% SDS-PAG. The proteins separated in the SDS-PAGE (SDS-PAG electrophoresis) were transferred to BioTrace nitrocellulose blotting membrane (PALL Life Sciences, Pensacola, FL, USA). The western blots were treated with blocking buffer, incubated with primary antibody, followed by development with alkaline phosphatase or enhanced chemiluminescence, as previously described (Yano et al., 2003). The blots were probed for the protein of interest with the proper primary antibody: rabbit or mouse anti-FLAG antibodies (Sigma-Aldrich, F3165-5MG, F7425-0.2MG), 1:2500 dilution; rabbit or mouse anti-Myc antibodies (GenScript, Piscataway, NJ, USA, A00704), 1:2000 dilution; rabbit anti-CBD2 (for the plasma membrane calcium ATPases), 1:5000 dilution; or mouse anti-α-tubulin (loading control) (Sigma-Aldrich, T6199), 1:10,000 dilution. Secondary antibodies were goat anti-mouse or rabbit conjugated to alkaline phosphatase or horse radish peroxidase used in a 1:10,000 dilution.

When the rabbit antibody was used for IP, the precipitated proteins were detected on western blot with the appropriate mouse primary antibody. When the mouse antibody was used for IP, a rabbit antibody was used for western blot analysis. For re-probing, the blots were incubated in the stripping buffer (50 mmol l^{-1} dithiothreitol, 50 mmol l^{-1} Tris HCl, 70 mmol l^{-1} SDS, pH 7) at 70°C for 30 min before washing in TBS-T (16 mmol l^{-1} Tris HCl, 4 mmol l^{-1} Tris, 137 mmol l^{-1} NaCl, 0.1% Tween 20, pH 7.5) and re-blocking and re-probing the blot as just described.

Mass spectrometry

We used mass spectrometry (MS) to confirm that the bands precipitated with anti-FLAG M2 affinity agarose from whole-cell

Journal of Experimental Biology (2016) 219, 3028-3038 doi:10.1242/jeb.141234

lysates of *PWA-FLAG*- and *PWB-FLAG*-expressing cells were FLAG-tagged PwA and PwB proteins, respectively. The precipitated proteins were separated on 12% SDS-PAGE. The gels were silver stained using the FAST Silver Kit (G-Biosciences, St Louis, MO, USA). The region corresponding to PwA- or PwB-FLAG was cut from the gel for MS analysis (see immediately below).

We examined whether the Ca_V1c channel could be immunoprecipitated with PwA from the P10 pellet in Fig. 2. Cultures of cells expressing both *FLAG-Ca$_V$1c* and *PWA-Myc* could not be cultured in sufficient quantities to analyze the results of IPs by western blots. Therefore, we used cells that grew better, i.e. expressing *FLAG-Ca$_V$1c* that had been transformed with untagged *PWA* expression plasmid. The P10 fraction was prepared from the cells expressing *PWA* and *FLAG-Ca$_V$1c* or *PWA* and the control *FLAG* epitope. The P10 fractions were normalized for protein concentration and solubilized with 1% Triton X-114 before centrifugation at 100,000 ***g***.

After centrifugation, we performed the IP from the resulting supernatant using anti-FLAG M2 affinity agarose using the method described above. The precipitated proteins were separated on 4–18% gradient SDS-PAGE. The resulting gel was silver stained and the regions corresponding to Ca_V1c (200–270 kDa) and PWA (20–30 kDa) were cut out. Each band was diced, destained in 30 mmol l^{-1} $K_3Fe(CN)_6$ and 100 mmol l^{-1} $Na_2S_2O_3$ in distilled water, and subjected to in-gel digestion with trypsin buffer (5% CH_3CN, 25 mmol l^{-1} NH_4HCO_3, 6 ng μl^{-1} trypsin) overnight at 37°C. The resulting peptides were analyzed by LC-MS/MS in an LTQ-XL linear ion trap mass spectrometer (Thermo Fisher Scientific) following the protocol of Yano and co-workers (Yano et al., 2013). The resulting protein data were searched simultaneously against the *Paramecium tetraurelia* forward (target) and reverse (decoy) peptide database (http://paramecium.cgm.cnrs-gif.fr/download/fasta/Ptetraurelia_peptides_v1.99.14.fasta) using Scaffold 4 (Proteome Software, Portland, OR, USA) with a precursor tolerance of 2 Da and a fragment ion tolerance of 0.5 Da. In our experience, the majority of cysteine residues following reducing conditions and SDS-PAGE are identified with an acrylamide adduction. For increased throughput and simplicity, we conducted searches with a static increase in 71.0 Da for acrylamide adduction. Differential modification of 16.0 Da on methionine residues was permitted. The search results were filtered using a delta correlation (dCn) score of 0.1 and cross-correlation (Xcorr) values of 1.9, 2.6, 3.2 and 3.4 for singly, doubly, triply and quadrupally charged ions, respectively. Proteins on these filtered lists that had two or more peptides were retained, and the false-positive ratio was zero in this list.

RT-PCR to evaluate the amounts of mRNA after RNAi treatment

Total RNA, first-strand cDNA and PCR were carried out as in Yano et al. (2003) and Valentine et al. (2012). Instead of serial cDNA dilution, PCR cycles were changed to 10, 15 and 20. See Fig. 3 for an example of the RT-PCR analysis that we carry out to determine whether the RNAi process is decreasing the mRNA of interest. We do not use this as a quantitative method. Note that the mRNA (cDNA) is not completely eliminated by RNAi.

Statistical tests

The backward swimming duration (s) values are shown as means±s.d. The Mann–Whitney *U*-test with two-tailed distribution was used for statistical analysis.

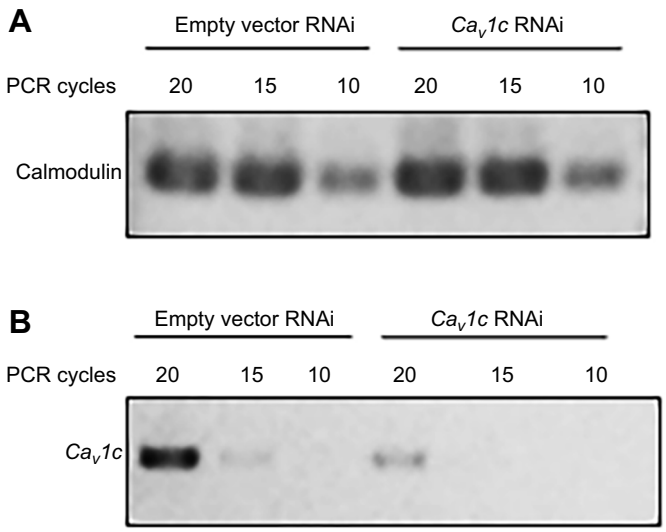

Fig. 3. Reduction of mRNA in RNAi-treated *P. tetraurelia* cells for *Ca$_V$1c* analyzed by RT-PCR. As a loading control to ensure the produced cDNA concentrations were approximately equal between test (*Ca$_V$1c*) and control (empty vector) RNAi-treated cells, calmodulin primers were used (Fig. S3A). We do not expect any changes in the mRNA levels of calmodulin in these RNAi-treated cells. The intensity of the bands gradually decreased as the number of PCR cycles decreased. No differences were observed in the bands between the test and control RNAi-treated cells, suggesting the cDNA of the two samples is approximately equal in concentration. We used primers to amplify *Ca$_V$1c* (see Fig. S3B). At 20 PCR cycles, the band from the *Ca$_V$1c* in the test cells is weaker than the band from the empty vector RNAi cells. By 15 cycles, the band for *Ca$_V$1c* in the test RNAi cells disappears while a band for *Ca$_V$1c* is still visible in the empty vector RNAi cells. Therefore, the transcript of *Ca$_V$1c* is reduced in the cells fed RNAi for *Ca$_V$1c* compared with the control fed cells, and is not due to differences in the starting cDNA concentrations. See Materials and methods for details.

RESULTS

Consensus domain analysis of three Ca_V channels in *Paramecium*

In our proteomic analysis of the *P. tetraurelia* ciliary membrane (Yano et al., 2013), peptides from the putative Ca_V1 α-subunit were identified. These Ca_V peptide sequences correspond to Ca_V1a, 1b and 1c. *Ca$_V$1a* and *Ca$_V$1b* are 87% identical at the nucleotide level and are likely to be derived from a recent whole genome duplication (WGD) (Aury et al., 2006). Their amino acid sequences are so close that the peptides we identified did not distinguish between Ca_V1a and 1b, but the peptides allowed us to establish that one or both of them are in the ciliary membrane. While *Ca$_V$1c* is 75% identical at the nucleotide level to *Ca$_V$1a* and *1b*, Ca_V1c can be distinguished from these other Ca_V proteins through peptides that we identified in our mass spectrometry analysis. The gene for *Ca$_V$1c* probably separated from the more ancient paralogs at the intermediate WGD and survived after the more recent WGD that created *Ca$_V$1a* and *1b* (Aury et al., 2006). A FLAG-tagged sequence for *Ca$_V$1c* was previously used to confirm the presence of the protein in cilia (Valentine et al., 2012; Yano et al., 2013).

Blast searches showed that Ca_V1a, 1b and 1c are most closely related to the $Ca_V\alpha1$ subunits from the mammalian subfamily called Ca_V1. When the *Paramecium* database was searched using the mouse and rat sequences for *Ca$_V$1.1* (NP_055008 for mouse and NP_446325 for rat) that are α1 subunits of typical high voltage-activated (L-type) channels, the *Paramecium* Ca_V1a, 1b and 1c have Expect (E) values of $6E^{-95}$, $8E^{-106}$ and $4E^{-98}$ to mammalian $Ca_V1.1$, respectively (see Table S1).

Journal of Experimental Biology (2016) 219, 3028-3038 doi:10.1242/jeb.141234

The *P. tetraurelia* ciliary Ca_V α-subunits share conserved domains with the sequences of the three vertebrate Ca_V subfamilies Ca_V1–3. Our analyses of predicted structure show that *P. tetraurelia* Ca_V1a, 1b and 1c all have the expected four copies of the ion transporting domain comprising six transmembrane domains (s1 to s6) and a pore loop in each unit (Tyson and Snutch, 2013) (Fig. 1). These four channel domains come together to form a highly charged selectivity filter that confers specificity for Ca^{2+} on the channel. The sequences found in the *P. tetraurelia* sequences have glutamic acids (E) in a critical position in each pore loop, giving these Ca_V α subunits the identity of the 'EEEE' motif in common with vertebrate Ca_V1 and 2, which are associated with high voltage-activated calcium channels. All CaV subgroups have transmembrane segments S3 and S4 that generally have an NxxD sequence and an R/KxxRxxxRxxR/K voltage sensor motif, respectively. The *P. tetraurelia* sequences likewise conserve these sequences (Fig. 1). The C termini of vertebrate Ca_V1 and 2 have a calmodulin binding motif and an IQ motif. Upon examination of the C termini, we found a putative calmodulin binding site in the C-terminal cytoplasmic region of *P. tetraurelia* Ca_V1a, 1b and 1c (Fig. 1). The cytoplasmic loop between domains I and II of *P. tetraurelia* Ca_V1a–c is very long (around 680 amino acids) as compared with that of the mammalian Ca_V1 and 2.

RNAi demonstrates that Ca_V1a–c contribute to ciliary reversal and backward swimming in depolarizing solutions

Backward swimming is known to depend upon an I_{CaV} in the cilia. The Ca^{2+} conductance is proportional to the duration of backward swimming induced by depolarization with high potassium (Haga et al., 1984; Hiwatashi et al., 1980). We used RNAi to examine whether reduction of Ca_V1a, 1b, 1c, or all three affected backward swimming, and, indirectly, whether their channel activities participate in the backward swimming behavior.

Segments of the *Ca_V1a*, *1b* and *1c* sequences (see Materials and methods) were amplified by PCR and sub-cloned into the RNAi vector L4440 for feeding RNAi. *Paramecium tetraurelia* cells were fed bacteria with the RNAi vector with the Ca_V insert or the empty RNAi vector (L4440) as a control. Cells were first tested in 30 mmol l^{-1} KCl in buffer to induce backward swimming after 24, 48 and 72 h of feeding on the RNAi bacteria, but changes in the backward swimming duration were most dramatic at 72 h of feeding. Therefore, we present here the data collected at 72 h of feeding RNAi. The RNAi with each *Ca_V1a*, *1b* or *1c* sequence individually caused significantly shorter backward swimming in high KCl compared with the control fed the empty vector (Mann–Whitney *U*-test; Fig. 4). Moreover, the RNAi for the mixture of *Ca_V1a*, *1b* and *1c* showed the shortest backward swimming as compared with the control or with RNAi for each individual calcium channel (Fig. 4).

Off-target effects by the RNAi sequences developed to downregulate *Ca_V1a–c* showed that the potential 23-mer nucleotide products from RNAi processing of the double-stranded RNA for *Ca_V1a* could bind many sequences within the mRNA for *Ca_V1b* and vice versa, marking these sequences for degradation (Table S3). However, there are very few potential off-target effects of *Ca_V1a* or *1b* on *Ca_V1c* and of *Ca_V1c* on either *Ca_V1a* or *1b*.

As a negative control for our RNAi of *Ca_V1a–c*, we carried out RNAi for gene sequence GSPATG00005636001, which has been identified previously (Ben-Johny et al., 2014; Taiakina et al., 2013) as a putative Ca_V channel α1-subunit based on sequence homology to mammalian $Ca_V1.1$. This putative Ca_V α-subunit has not been found in the proteomic analysis of the ciliary membrane. RNAi for this sequence does not reduce backward swimming (Fig. 5) as seen for the RNAi of *Ca_V1a*, *1b* or *1c* shown in Fig. 4.

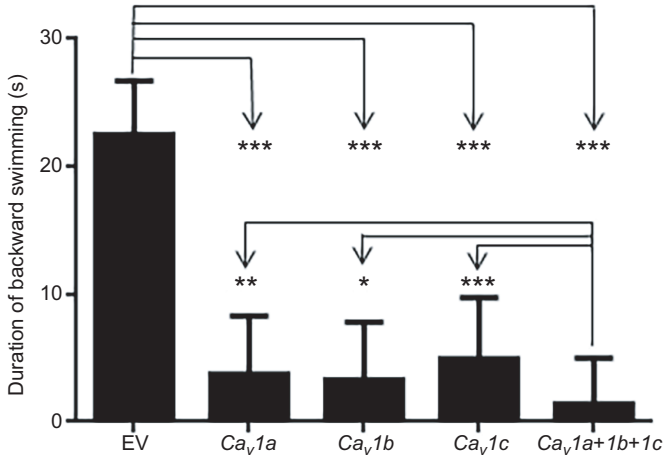

Fig. 4. Effect of RNAi for *$Ca_V\alpha1$* genes (*Ca_V1a*, *1b* and *1c*) on the duration of backward swimming under the depolarization condition of 30 mmol l^{-1} KCl in *P. tetraurelia*. The duration of backward swimming times (s; mean± s.d.) was measured for RNAi experiments of wild-type cells fed bacteria with the empty vector (EV) (22.5±4.2 s, *n*=80), the vector with a sequence from *Ca_V1a* (3.7±4.6 s, *n*=46), *Ca_V1b* (3.3±4.5 s, *n*=45) or *Ca_V1c* (4.9±4.8 s, *n*=45), and from all three, *Ca_V1a*, *1b* and *1c* (*1a+1b+1c*; 1.4±4.8 s, *n*=85). RNAi for *Ca_V1a*, *b* or *c* reduced the duration of backward swimming compared with RNAi for EV (***P<0.001, Mann–Whitney *U*-test, two tailed). RNAi using a mixture of three RNAi bacteria reduced the backward swimming further than RNAi for the individual genes (*P<0.05, **P<0.01, ***P<0.001). Arrows indicate the pair-wise comparisons made for statistical testing.

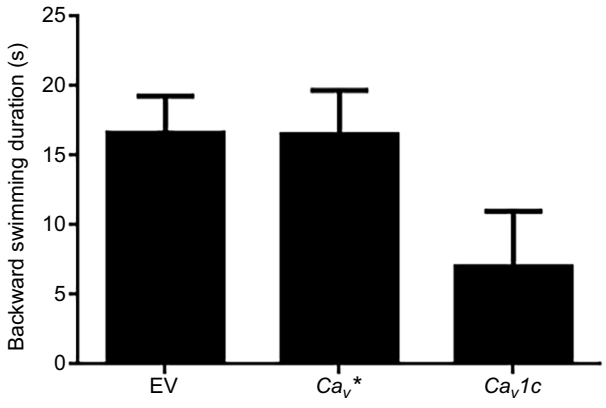

Fig. 5. Effect of RNAi for *Ca_V1c* and GAPATG00005636001 (*Ca_V) on the backward swimming duration under the depolarizing condition of 30 mmol l^{-1} KCl in *P. tetraurelia*.** Reduction of *Ca_V1c* using RNAi was used as a positive control and, as in Fig. 1, showed much shorter backward swimming compared with control empty vector RNAi cells. RNAi for sequence GSPATG0005636001 (*Ca_V**), which had been identified by others (Taiakina et al., 2013; Ben-Johny et al., 2014) as a putative voltage-gated calcium channel based on sequence homology to mammalian $Ca_V1.1$, does not show any reduction in backward swimming duration [values for these histograms are empty vector (EV) 16.8±2.7 s, *n*=181 versus GSPATG0005636001 (*Ca_V**) 16.5±3.2 s, *n*=181, P>0.05, Mann–Whitney *U*-test]. The backward swimming time for Ca_V1c is 7.0±4.0 s, *n*=102.

Journal of Experimental Biology (2016) 219, 3028-3038 doi:10.1242/jeb.141234

Wild-type *PW* gene sequences rescue the wild-type phenotype when injected into *pw* cells, but overexpression of Ca_V1a, *1b* or *1c* does not

Haynes and others have shown that injection of the wild-type sequence for *PWA* or *PWB* into the mutant cell nucleus will rescue the wild-type phenotype (Haynes et al., 2000, 1998). In order to carry out the present study, we reproduced the outcome that the wild-type *PW* sequences could rescue the wild-type phenotype, i.e. restore the ability of *pw* cells to swim backward in depolarizing solutions. Table S5 shows that injection of the wild-type *PWA* or *PWB* sequence restores the ability of *pwA* or *pwB* mutants, respectively, to swim backward in 8 mmol l^{-1} $BaCl_2$, although the duration is not as long as the backward swimming of wild-type controls. The *PWA* or *PWB* sequences with epitope tags similarly restore the ability of *pwA* or *pwB* mutant cells to swim backward in 8 mmol l^{-1} $BaCl_2$ solutions (Table S5).

In contrast, expression of *FLAG-*Ca_V1a, *1b* or *1c* in *pwA* or *pwB* cells does not result in the restoration of backward swimming tested in 30 mmol l^{-1} KCl solutions (Table S5). Even with these additional exogenous sequences for Ca_V1a, *1b* or *1c* injected into the *pw* cells, the wild-type phenotype is not rescued in *pw* mutants.

Ca_V1a, 1b and 1c proteins are found in cilia, but *pw* mutants do not show these Ca_V1s in cilia unless they are rescued by expression of the wild-type *PW* sequence

The FLAG-tagged Ca_V1c can be immunoprecipitated from the ciliary membrane of wild-type cells (Fig. 6A) and its expression in wild-type cells increases their backward swimming (Table S5). Similarly, FLAG-Ca_V1a or 1b were immunoprecipitated from the ciliary membrane of wild-type cells expressing *FLAG-*Ca_V1a or *1b*, respectively (Fig. S1). However, the cells expressing tagged Ca_V1a or *1b* showed the same backward swimming duration as the control cells (Table S5). The expression of the tagged Ca_V1s' proteins in wild-type cilia made it possible for us to investigate the possibility that the *pw* mutants do not activate the Ca_V1s to initiate backward swimming because the Ca_V1s are not in their cilia.

FLAG-Ca_V1c was expressed in mutant *pw* cells or in *pw* cells whose phenotypes had been rescued with wild-type *PW* sequences (Fig. 6A). In each case, the cells were tested for restoration of backward swimming before the cilia were isolated from transformed cells. The isolated cilia were treated with 1% Triton X-114 and the proteins were precipitated using anti-FLAG M2 affinity agarose, then analyzed by western blot. Note that in lane C of both *pwA* and *pwB* cells shown in Fig. 6A, the FLAG-Ca_V1c is not immunoprecipitated from the cilia of *pwA* or *pwB* cells co-expressing only the pPXV plasmid. However, once the *pw* mutants are rescued with the wild-type sequence for *PWA* or *PWB*, the FLAG-Ca_V1c protein can be immunoprecipitated from the cilia (lane T of *pwA* and *pwB* cells in Fig. 6A).

As a concentration control for Fig. 6A, the plasma membrane calcium ATPases 2, 3 and 4 (PMCA) (CR932147, CR932150 and CR933346) were precipitated from the cilia with anti-CBD2 antibody (Van Houten, 1998). The western blot showed that the intensity of bands corresponding to the PMCAs were almost the

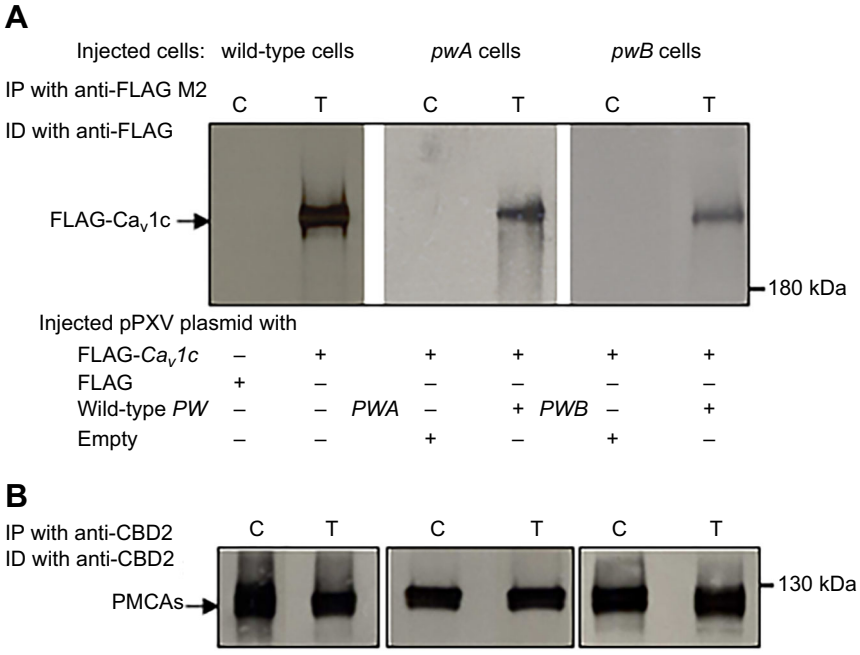

Fig. 6. Wild-type *PWA* and *PWB* genes are required for the presence of Ca_V1c in cilia of *P. tetraurelia*. (A) Cilia isolated from wild-type (51s), *pwA* and *pwB* mutant cells expressing *FLAG-*Ca_V1c (lane T) or only *FLAG* (lane C) were solubilized with 1% Triton X-114. The FLAG-Ca_V1c that was precipitated with anti-FLAG M2 was detected with anti-FLAG polyclonal antibody on western blots. The *pwA* cells expressing both *FLAG-*Ca_V1c and the *PWA* gene show backward swimming, i.e. the wild-type phenotype is rescued (Table S5). However, the *pwA* cells expressing only *FLAG-*Ca_V1c do not show backward swimming, i.e. the *pwA* mutants are not rescued (Table S5). The band corresponding to FLAG-Ca_V1c (arrow) was detected in the ciliary membrane of *pwA* cells expressing both *FLAG-*Ca_V1c and the *PWA* protein (lane T), but not in the cilia of *pwA* mutant cells expressing only *FLAG-*Ca_V1c (lane C). Similarly, *pwB* cells expressing *FLAG-*Ca_V1c show no backward swimming in depolarizing solutions (Table S5), while the *pwB* mutant cells expressing both *FLAG-*Ca_V1c and *PWB* are capable of swimming backward (Table S5). The band corresponding to FLAG-Ca_V1c was detected in the ciliary membrane of *pwB* mutant cells that express both the FLAG-Ca_V1c and PwB protein (lane T), but not in the ciliary membrane from *pwB* cells that express only the FLAG-Ca_V1c protein (lane C). IP, immunoprecipitation; ID, immunodevelopment. (B) Loading control. After IP with anti-FLAG, plasma membrane calcium ATPases (PMCAs) were precipitated with anti-CBD2, which was produced against the calmodulin binding domain of the *Paramecium* plasma membrane calcium ATPase 2 (Van Houten, 1998). The PMCAs were detected with anti-CBD2 in lanes C (control) and T (test). Approximately the same amount of PMCA seems to be solubilized in the ciliary sample of control and test cells with 1% Triton X-114.

Journal of Experimental Biology (2016) 219, 3028-3038 doi:10.1242/jeb.141234

same between the cilia of cells expressing the *FLAG-Ca$_V$1c* and control vector pPXV, and the cilia co-expressing *FLAG-Ca$_V$1c* and the *PWA* or *PWB* wild-type gene (Fig. 6B).

Similar results were obtained when the tagged channel genes for *Ca$_V$1a* and *1b* were co-expressed with the wild-type *PWA* in *pwA* cells or *PWB* gene in *pwB* cells. Under these conditions, FLAG-Ca$_V$1a and 1b proteins could be immunoprecipitated from the cilia of *pwA* or *pwB* cells (see Fig. S1).

Subcellular localization of PwA and PwB proteins, and potential interaction with Ca$_V$1c

The injection of cytoplasm, especially fraction P10 (see Fig. 2 and Materials and methods), from the wild-type cells into the *pwA* or *pwB* cells caused the mutants to regain the voltage-activated calcium conductance without new protein synthesis (Haga et al., 1984). Therefore, we included in our determination of the subcellular localization of Pw proteins the P10 fraction used by Haga and co-workers to cure *pw* phenotypes (Haga et al., 1984) and also the P2 fraction, because both fractions were reported to be enriched in ER (Haga et al., 1984; Wright and Van Houten, 1990).

We used western blots to locate Pw proteins in cell fractions. Fig. 7A shows western blots of the P2 fraction and the pellicle, and western blots of IPs from the cilia of *pwA* cells expressing *PwA-FLAG* (test, T lane) or *FLAG* (control, C lane) (see Materials and methods). We considered bands to be from PwA-FLAG only if they were found in T lanes and not C lanes, as only the T lanes should have the expressed tagged protein. The blots of the P2 fraction show three bands (30, 27 and 25 kDa) in the T lane and one (30 kDa, blue arrow) in the C lane. We discounted the 30 kDa band from further analysis because it was in both the T and C lanes. The P2 band at 27 kDa (upper black arrow, T lane only) matches the expected size of the PwA-FLAG protein. The P2 band of 25 kDa (lower black arrow, T lane only) matches the PwA-FLAG protein without the signal sequence.

Blots of the pellicles of cells expressing *PwA-FLAG* and *FLAG* show three bands of 25, 27 and 28 kDa in the T lane only. The pellicle band of 28 kDa (arrowhead) matches a glycosylated form of the PwA-FLAG protein, which has two putative glycosylation sites. The lower band in the pellicle blot at 25 kDa matches the predicted size of PwA-FLAG without the signal sequence. In the blot from the IP of PwA-FLAG from cilia, two bands of 25 and 28 kDa were detected in the T lane only, similar to the pellicle western blot.

Proteins were immunoprecipitated with anti-FLAG M2 from the Triton-114 extracts of P2, P10, pellicle and cilia from *pwB* cells expressing *PWB-FLAG* (T lane) or *FLAG* (C lane; Fig. 7B). Western blots show bands at 35 kDa in the T lane for the P2 and P10 fractions (Fig. 7B, black arrow), which are consistent with PwB-FLAG protein. The PwB-FLAG protein was not found in the pellicle or cilia IPs.

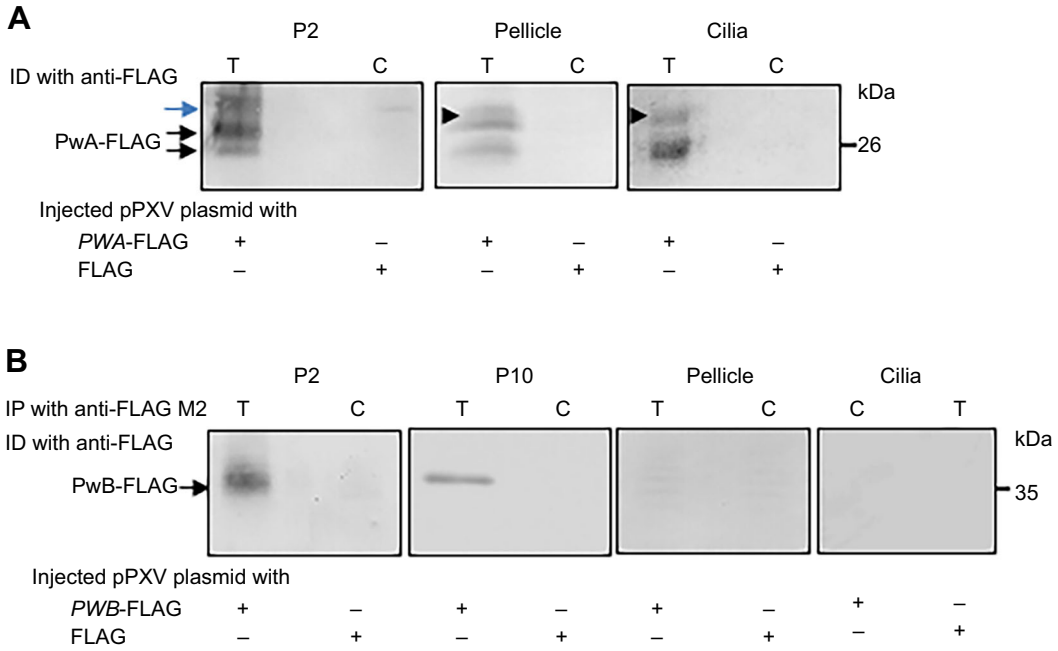

Fig. 7. Subcellular localization of Pawn A (PwA) and Pawn B (PwB) proteins in *P. tetraurelia*. To identify the subcellular locations of Pawn proteins, we examined cellular fractions for the presence of FLAG-tagged Pawn proteins by western blotting of the fractions directly or of immunoprecipitations from the fractions. (A) Western blots of the P2 subcellular fraction and the pellicle, and of IP from the cilia of *pwA* cells expressing *PwA-FLAG* (test, T) or *FLAG* (control, C), were analyzed with an anti-FLAG antibody (see Materials and methods). In the western blot of the proteins of the P2 fraction (not an IP), there were three bands (30, 27 and 25 kDa) in lane T and one band of 30 kDa in lane C. Because the band of 30 kDa (blue arrow) is in lane C, we believe that it is from recognition of a FLAG epitope by the antibody, but not of the PwA-FLAG protein, which should be found only in lane T. Therefore, this 30 kDa band, although found in lane T, is not a form of the PwA protein. The P2 band at 27 kDa (in lane T only) is consistent with the expected size of the PwA-FLAG protein (upper black arrow). The P2 band of 25 kDa (in lane T only) is consistent with the PwA-FLAG protein without the signal sequence (lower black arrow). In the blot of pellicle proteins, three bands of 25, 27 and 28 kDa were detected in lane T only; in the blot of cilia proteins, two bands of 25 and 28 kDa were detected in lane T only. The pellicle and cilia bands of 28 kDa (arrowheads) are consistent with a glycosylated form of the PwA-FLAG protein, as PwA has two putative glycosylation sites. The bands at 27 kDa are consistent with the expected size of the PwA-FLAG protein, and the bands at 25 kDa are consistent with the PwA-FLAG protein with the signal sequence removed. (B) The proteins immunoprecipitated with anti-FLAG M2 from Triton X-114 extracts of P2, P10, pellicle and cilia from the *pwB* cells expressing *PwB-FLAG* (lane T) or *FLAG* (lane C) were analyzed by western blot. The bands at 35 kDa in lane T of blots from the P2 and P10 fractions (arrow) are consistent with the expected mass of the PwB-FLAG protein. The PwB-FLAG protein was not identified in the pellicle or cilia IPs.

Journal of Experimental Biology (2016) 219, 3028-3038 doi:10.1242/jeb.141234

To examine whether the PwB protein interacts (directly or indirectly) with Ca_V1c in the P10 fraction, we carried out reciprocal IPs of FLAG-tagged Ca_V1c and PwB-Myc proteins expressed in wild-type cells. Fig. 8A,B shows the western blot results of reciprocal IPs of FLAG-Ca_V1c and PwB-Myc proteins from the P10 fraction. After the IP with the anti-Myc beads, a FLAG-Ca_V1c band of 250 kDa was detected in lane T (Fig. 8A). As expected, the PwB-Myc protein of 35 kDa was also detected. From the IP with anti-FLAG M2 affinity agarose, the PwB-Myc protein was detected at 35 kDa (Fig. 8B). The loading control is shown in Fig. 8C,D.

To examine whether the PwA protein interacts with FLAG-Ca_V1c in the P10 fraction, FLAG-Ca_V1c and PwA-Myc (test) and empty vectors containing FLAG and Myc (control) were co-expressed in wild-type cells. We could not grow the *PWA-Myc* transformed cells to sufficient density for the IPs, which led us to look for the presence of the PwA protein by overexpressing the untagged version and using MS to examine the gel of the IP products. IP with anti-FLAG was carried out, and the immunoprecipitated proteins were analyzed by separating the precipitate into a sample for a blot to confirm the successful IP of Ca_V1c and a sample for a silver-stained gel that would be analyzed by MS/MS. Two regions, 200–270 kDa and 20–30 kDa, corresponding to Ca_V1c and PwA proteins, respectively, were cut out from the silver-stained gel (Fig. 9) and analyzed by MS. The same experiments were repeated three times. Although the peptides of Ca_V1c were detected from the regions corresponding to FLAG-Ca_V1c, no peptides from the PwA protein were detected.

DISCUSSION

The power stroke of the cilia of *P. tetraurelia* is controlled by the activity of the Ca_V channels in the ciliary membrane. Through proteomic analysis of the ciliary membrane, we found three proteins and their corresponding genes that could potentially be responsible for the action potential that controls the ciliary beat form (Yano et al., 2013). The cloning and epitope tagging of these large genes was challenging, but allowed us to demonstrate that the proteins from the expression vectors were located in the ciliary membrane. The first channel, Ca_V1c, was the first of three that we cloned and expressed (Valentine et al., 2012). The expressed Ca_V1a and 1b channels are shown in the present study. The epitope tags allowed us to surmount the challenge of immunoprecipitating these large proteins to concentrate them for definitive identification in wild-type and rescued *pwA* and *pwB* mutants.

Using RNAi, we were able to downregulate the expression of the *Ca_V1a*, *1b* and *1c* genes singly and together to demonstrate that

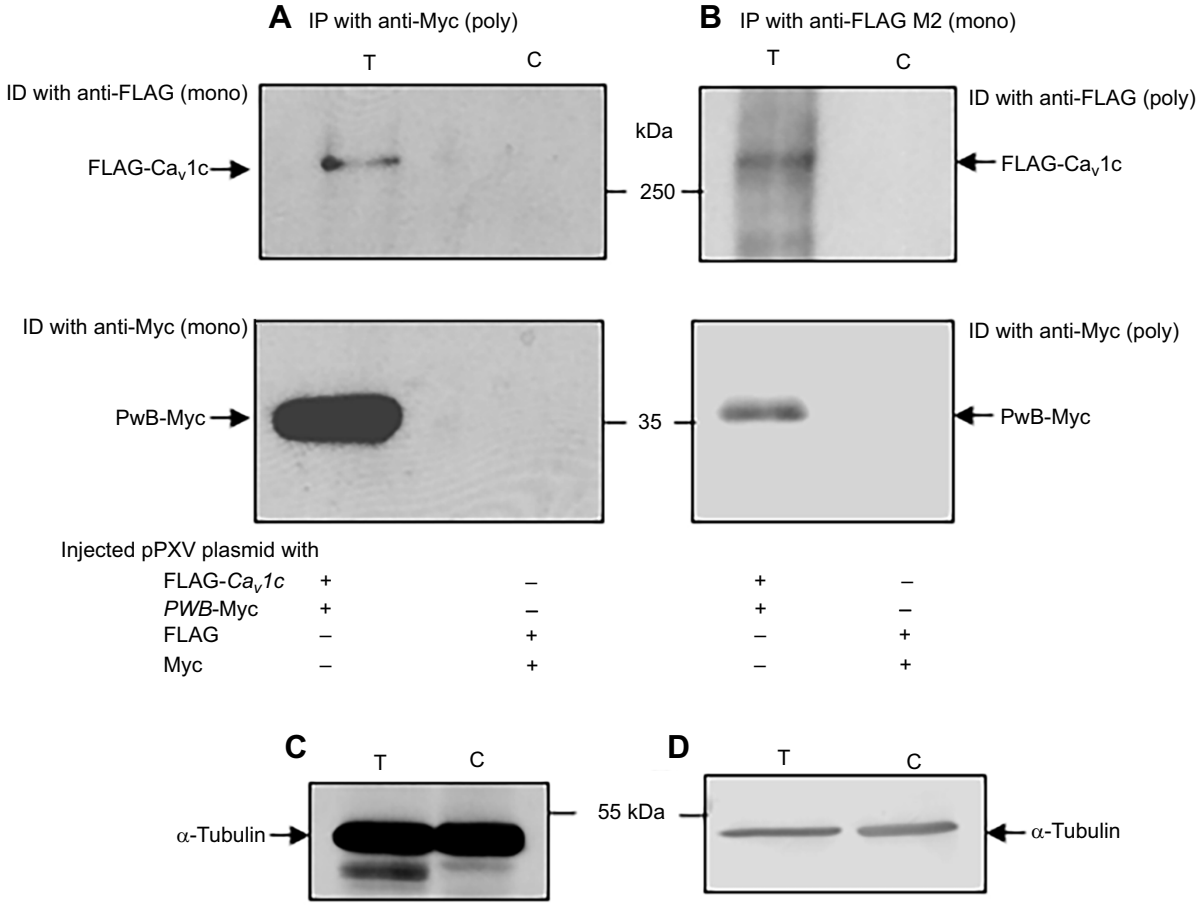

Fig. 8. Reciprocal immunoprecipitation for Ca_V1c and PwB protein in *P. tetraurelia*. (A,B) The subcellular P10 fraction from cells expressing *FLAG-Ca_V1c* and *PwB-Myc* (T) or *FLAG* and *Myc* (C) was solubilized with Triton X-114. The tagged proteins were precipitated with anti-FLAG M2 or anti-Myc polyclonal antibody, and analyzed on western blots. From the IP with anti-Myc polyclonal antibody (Fig. 8A), the band (~250 kDa) for the FLAG-Ca_V1c protein was detected in lane T with anti-FLAG monoclonal antibody, but not in lane C. As expected, the band (35 kDa) for the PwB-Myc protein was detected with anti-Myc monoclonal antibody. From the IP with anti-FLAG M2 (Fig. 8B), the band for the FLAG-Ca_V1c protein was detected in lane T with the anti-FLAG polyclonal antibody. The band for the PwB-Myc protein was detected in lane T with anti-Myc polyclonal antibody, but not in lane C. (C,D) Loading control. Before the IP with anti-FLAG, a small amount (20 µl) of the clarified lysate (see Materials and methods) was removed from the test and control samples and analyzed by western blot probed using anti-α-tubulin to demonstrate that the test and control samples contained approximately the same amount of protein.

Journal of Experimental Biology (2016) 219, 3028-3038 doi:10.1242/jeb.141234

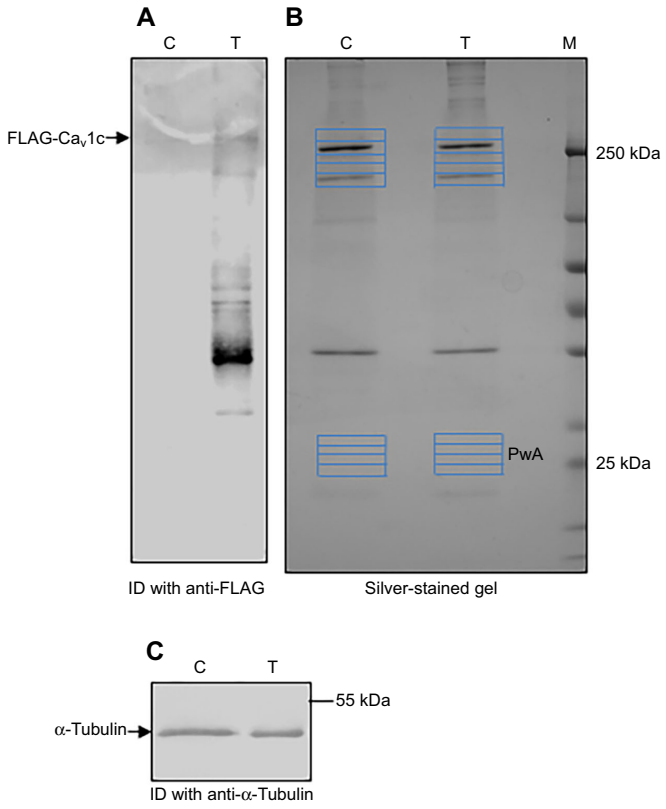

Fig. 9. Western blot and silver-stained gel from IP with anti-FLAG M2 affinity agarose in *P. tetraurelia*. We examined whether the PwA protein was co-precipitated from the IP with anti-FLAG M2 affinity agarose for the FLAG-Ca_V1c channel using mass spectrometry (MS) analysis. The P10 fraction from cells expressing *FLAG-Ca$_V$1a* and *PWA* (lane T) or only *FLAG* and empty vector (lane C) were solubilized with 1% Triton X-114, and the Triton X-114 extract was used for IP. (A) Ten percent of the precipitated protein was analyzed by western blot. The bands of FLAG-Ca_V1a were detected with anti-FLAG antibody (arrows). (B) The remaining protein was analyzed by silver stain. The areas corresponding to Ca_V1a (200–270 kDa) and PwA (20–30 kDa) were cut out from the gel and used for MS analysis. Lane M shows the protein molecular weight marker. (C) The same amount of Triton extract was used as a loading control. α-Tubulin was detected by anti-α-tubulin antibody and serves as a control for the protein solubilized in both the test and control samples.

these Ca_V α-subunits contribute to the action potential that causes the cells to turn. RNAi generally does not cause a complete removal of a protein as a null mutation would. The mRNA for these channels is not eliminated by RNAi, as shown by RT-PCR (Fig. 3). However, the extreme reduction of backward swimming by RNAi treatment, especially that seen in the cells depleted of all three Ca_V1a–c channels, gives us confidence that these channels are the major, if not the only, contributors to the calcium action potential.

Another related sequence not found in the cilia by proteomics was used as an RNAi control. Downregulation of the expression from this gene had no effect on the depolarization-induced backward swimming (Fig. 5).

We turned to the *pw* mutants for additional evidence that the presence of the Ca_V1a–c proteins in cilia correlates with the action potential and depolarization-induced backward swimming. In addition, the techniques of tagging and immunoprecipitation of the large channels allowed us to address the very old question of the cause of the failure of Pawn *pwA* and *pwB* mutants to show a calcium conductance upon depolarization that would normally elicit an action potential and backward swimming in the wild type.

Pawn mutants, *pwA*, *pwB* and *pwC*, were first described in 1969 (for a history, see Kung, 1971). Electrophysiological studies showed that Pawns lack the $I_{Ca(V)}$ current, but otherwise have normal K^+ and other conductances (Satow and Kung, 1974, 1980). Between 1998 and 2000, the *PWA* and *PWB* genes of the *pwA* and *pwB* mutants were cloned by complementation, but neither appeared to code for a Ca_V α or ancillary subunit (Haynes et al., 2000, 1998) (the gene for the *pwC* mutant remains unidentified). It had been shown that if the ciliary membrane were bypassed, and Ca^{2+} had access to the axoneme, *pwA* and *pwB* cells could beat their cilia with the reversed power stroke. However, when the ciliary membrane was intact, they could not (Kung and Naitoh, 1973). These experiments demonstrated that the axonemes of *pw* cells were functional. More recent experiments showed that the Ca^{2+} in cilia that enters through the Ca_V channels of wild-type cells does not spill into the cell body to trigger the Ca^{2+}-dependent exocytosis of trichocysts, but that strong chemically induced exocytosis that is dependent upon a burst of Ca^{2+} released from intracellular stores could elicit the reversal of the ciliary beat, that is, reach the axoneme (Husser et al., 2004). While *pw* cells could not reverse their ciliary beating with depolarization, the strong chemically induced exocytosis could sweep enough Ca^{2+} into the cilia to cause a ciliary reversal. These results are consistent with the observations of Kung and Naitoh (1973) that the *pw* cell's axonemes were functional if Ca^{2+} could reach them.

It was not known whether intact *pwA* and *pwB* mutants did not reverse their beat because they lacked the Ca_V channels in their cilia or whether the *pw* mutants had Ca_V channels in their ciliary membranes but these channels could not be activated with depolarization. In the present study, we could not find the Ca_V1a–c expressed channels in the ciliary membranes of Pawn mutants *pwA* or *pwB*, suggesting that these mutants cannot swim backward for lack of the Ca^{2+} current from the channels. Expressing the genes for these channels in the mutants did not restore the ability to reverse ciliary beating and these expressed channels could not be found in the ciliary membrane. However, restoring the wild-type versions of the *PWA or PWB* mutant genes not only restores the ability to reverse swimming, but also restores the Ca_V1a–c channels in the ciliary membrane. These results reinforce our contention that the presence of one of the channel types Ca_V1a, b or c is necessary and perhaps sufficient for backward swimming.

The Pawn proteins do not resemble vertebrate Ca_V channel α1 or other subunits that are thought to assist in trafficking of the vertebrate Ca_V α-subunits to the cell surface (Dolphin, 2012). However, they appear to be involved in trafficking the *P. tetraurelia* Ca_V1a–c proteins to the ciliary membrane. Because the PwB protein appears to be limited to the ER, its role in trafficking may be to assist the channels to reach the proper ER–Golgi pathway. The PwB and Ca_V1c proteins can be reciprocally immunoprecipitated, implicating an interaction (direct or indirect) between the two proteins that is sufficiently strong to survive immunoprecipitation. The PwA protein, while found in the ER, surface membranes and cilia, does not have a similarly strong interaction. Nonetheless, it appears to be crucial in guiding the Ca_V1a–c channels to the cilia.

Previously, we showed that other channels of the *P. tetraurelia* ciliary membrane, a calcium-activated K^+ channel (SK1a) and polycystin-2 (PKD2), require Bardet–Biedel syndrome (BBS) proteins to traffic into the cilia (Valentine et al., 2012). In that same study, we found that Ca_V1c did not require the BBS8 protein of the BBSome complex to successfully reach the ciliary membrane.

Acknowledgements
We thank Dr Y. W. Lam for analyzing the mass spectrometry data.

Competing interests
The authors declare no competing or financial interests.

Author contributions
S.L., J.Y. and J.L.V.H. designed and conducted the study. S.L. and J.Y. carried out all laboratory work and performed data analysis. J.L.V.H. and M.S.V. wrote the manuscript with contributions from J.Y.

Funding
Research reported in this publication was supported by an Institutional Development Award (IDeA) from the National Institute of General Medical Sciences (NIGMS) of the National Institutes of Health (NIH) under grant number P20GM103449 to J.L.V.H. Its contents are solely the responsibility of the authors and do not necessarily represent the official views of NIGMS or NIH. Deposited in PMC for release after 12 months.

Supplementary information
Supplementary information available online at
http://jeb.biologists.org/lookup/doi/10.1242/jeb.141234.supplemental

References

Aury, J.-M., Jaillon, O., Duret, L., Noel, B., Jubin, C., Porcel, B. M., Ségurens, B., Daubin, V., Anthouard, V., Aiach, N. et al. (2006). Global trends of whole-genome duplications revealed by the ciliate *Paramecium tetraurelia*. *Nature* **444**, 171-178.
Ben-Johny, M., Yang, P. S., Niu, J., Yang, W., Joshi-Mukherjee, R. and Yue David, T. (2014). Conservation of Ca^{2+}/calmodulin regulation across Na and Ca^{2+} channels. *Cell* **157**, 1657-1670.
Berbari, N. F., O'Connor, A. K., Haycraft, C. J. and Yoder, B. K. (2009). The primary cilium as a complex signaling center. *Curr. Biol.* **19**, R526-R535.
Bloodgood, R. A. (2010). Sensory reception is an attribute of both primary cilia and motile cilia. *J. Cell Sci.* **123**, 505-509.
Blum, M. and Vick, P. (2015). Left-right asymmetry: cilia and calcium revisited. *Curr. Biol.* **25**, R205-R207.
Brenker, C., Goodwin, N., Weyand, I., Kashikar, N. D., Naruse, M., Krähling, M., Müller, A., Kaupp, U. B. and Strünker, T. (2012). The CatSper channel: a polymodal chemosensor in human sperm. *EMBO J.* **31**, 1654-1665.
DeCaen, P. G., Delling, M., Vien, T. N. and Clapham, D. E. (2013). Direct recording and molecular identification of the calcium channel of primary cilia. *Nature* **504**, 315-318.
Delling, M., DeCaen, P. G., Doerner, J. F., Febvay, S. and Clapham, D. E. (2013). Primary cilia are specialized calcium signalling organelles. *Nature* **504**, 311-314.
Delling, M., Indzhykulian, A. A., Liu, X., Li, Y., Xie, T., Corey, D. P. and Clapham, D. (2016). Primary cilia are not calcium-responsive mechanosensors. *Nature* **531**, 656-660.
Doerner, J. F., Delling, M. and Clapham, D. E. (2015). Ion channels and calcium signaling in motile cilia. *eLife* **4**, e11066.
Dolphin, A. (2012). Calcium channel auxiliary alpha-two-delta and beta subunits: trafficking and one step beyond. *Nat. Rev. Neurosci.* **13**, 542-555.
Dunlap, K. (1977). Localization of calcium channels in *Paramecium caudatum*. *J. Physiol.* **271**, 119-133.
Eckert, R. (1972). Bioelectric control of ciliary activity. *Science* **176**, 473-481.
Fujiu, K., Nakayama, Y., Yanagisawa, A., Sokabe, M. and Yoshimura, K. (2009). *Chlamydomonas* CAV2 encodes a voltage-dependent calcium channel required for the flagellar waveform conversion. *Curr. Biol.* **19**, 133-139.
Fujiu, K., Nakayama, Y., Iida, H., Sokabe, M. and Yoshimura, K. (2011). Mechanoreception in motile flagella of *Chlamydomonas*. *Nat. Cell Biol.* **13**, 630-632.
Haga, N., Forte, M., Saimi, Y. and Kung, C. (1982). Microinjection of cytoplasm as a test of complementation in *Paramecium*. *J. Cell Biol.* **92**, 559-564.
Haga, N., Forte, M., Saimi, Y. and Kung, C. (1984). Characterization of cytoplasmic factors which complement Ca^{2+} channel mutations in *Paramecium tetraurelia*. *J. Neurogenet.* **1**, 259-274.
Haynes, W. J., Ling, K.-Y., Saimi, Y. and Kung, C. (1995). Induction of antibiotic-resistance in *Paramecium tetraurelia* by the bacterial gene APH-3'-II. *J. Eukaryot. Microbiol.* **42**, 83-91.
Haynes, W. J., Vaillant, B., Preston, R. R., Saimi, Y. and Kung, C. (1998). The cloning by complementation of the pawn-A gene in *Paramecium*. *Genetics* **149**, 947-957.
Haynes, W. J., Ling, K.-Y., Preston, R. R., Saimi, Y. and Kung, C. (2000). The cloning and molecular analysis of pawn-B in *Paramecium tetraurelia*. *Genetics* **155**, 1105-1117.
Hiwatashi, K., Haga, N. and Takahashi, M. (1980). Restoration of membrane excitability in a behavioral mutant of *Paramecium caudatum* during conjugation and by microinjection of wild-type cytoplasm. *J. Cell Biol.* **84**, 476-480.
Huang, K., Diener, D. R., Mitchell, A., Pazour, G. J., Witman, G. B. and Rosenbaum, J. L. (2007). Function and dynamics of PKD2 in *Chlamydomonas reinhardtii* flagella. *J. Cell Biol.* **179**, 501-514.
Husser, M. R., Hardt, M., Blanchard, M.-P., Hentschel, J., Klauke, N. and Plattner, H. (2004). One-way calcium spill-over during signal transduction in *Paramecium* cells: from the cell cortex into the cilia, but not in the reverse direction. *Cell Calcium* **36**, 349-358.
Kleene, S. J. (2008). The electrochemical basis of odor transduction in vertebrate olfactory cilia. *Chem. Senses* **33**, 839-859.
Kleene, S. J. and Van Houten, J. L. (2014). Electrical signaling in motile and primary cilia. *Bioscience* **64**, 1092-1102.
Kung, C. (1971). Genic mutants with altered system of excitation in *Paramecium aurelia*. II. Mutagenesis, screening and genetic analysis of the mutants. *Genetics* **69**, 29-45.
Kung, C. and Naitoh, Y. (1973). Calcium-induced ciliary reversal in the extracted models of 'Pawn', a behavioral mutant of *Paramecium*. *Science* **179**, 195-196.
Kung, C. and Saimi, Y. (1982). The physiological basis of taxes in *Paramecium*. *Annu. Rev. Physiol.* **44**, 519-534.
Lee, K. L., Guevarra, M. D., Nguyen, A. M., Chua, M. C., Wang, Y. and Jacobs, C. R. (2015). The primary cilium functions as a mechanical and calcium signaling nexus. *Cilia* **4**, 7.
Lishko, P. and Kirichok, Y. (2015). Signaling the differences between cilia. *eLife* **4**, e12760.
Machemer, H. (1988). *Electropysiology*. Berlin: Springer-Verlag.
Machemer, H. and Ogura, A. (1979). Ionic conductances of membranes in ciliated and deciliated *Paramecium*. *J. Physiol.* **296**, 49-60.
McRory, J. E., Santi, C. M., Hamming, K. S. C., Mezeyova, J., Sutton, K. G., Baillie, D. L., Stea, A. and Snutch, T. P. (2001). Molecular and functional characterization of a family of rat brain T-type calcium channels. *J. Biol. Chem.* **276**, 3999-4011.
Mikami, A., Imoto, K., Tanabe, T., Niidome, T., Mori, Y., Takeshima, H., Narumiya, S. and Numa, S. (1989). Primary structure and functional expression of the cardiac dihydropyridine-sensitive calcium channel. *Nature* **340**, 230-233.
Pazour, G. J. and Witman, G. B. (2003). The vertebrate primary cilium is a sensory organelle. *Curr. Opin. Cell Biol.* **15**, 105-110.
Pifferi, S., Boccaccio, A. and Menini, A. (2006). Cyclic nucleotide-gated ion channels in sensory transduction. *FEBS Lett.* **580**, 2853-2859.
Sasner, J. M. and Van Houten, J. L. (1989). Evidence for *Paramecium* folate chemoreceptor. *Chem. Senses* **14**, 587-595.
Satow, Y. and Kung, C. (1974). Genetic dissection of active electrogenesis in *Paramecium aurelia*. *Nature* **247**, 69-71.
Satow, Y. and Kung, C. (1980). Ca-induced K^+ outward current in *Paramecium tetraurelia*. *J. Exp. Biol.* **88**, 293-303.
Singla, V. and Reiter, J. (2006). The primary cilium as the cell's antenna: signaling at a sensory organelle. *Science* **313**, 629-633.
Starr, T. V., Prystay, W. and Snutch, T. P. (1991). Primary structure of a calcium channel that is highly expressed in the rat cerebellum. *Proc. Natl. Acad. Sci. USA* **88**, 5621-5625.
Taiakina, V., Boone, A. N., Fux, J., Senatore, A., Weber-Adrian, D., Guillemette, J. G. and Spafford, J. D. (2013). The calmodulin-binding, short linear motif, NSCaTE is conserved in L-type channel ancestors of vertebrate Cav1.2 and Cav1.3 channels. *PLoS ONE* **8**, e61765.
Tyson, J. R. and Snutch, T. P. (2013). Molecular nature of voltage-gated calcium channels: structure and species comparison. *Wiley Interdiscip. Rev. Membr. Transp. Signal.* **2**, 181-206.
Valentine, M. S., Rajendran, A., Yano, J., Weeraratne, S. D., Beisson, J., Cohen, J., Koll, F. and Van Houten, J. (2012). *Paramecium* BBS genes are key to presence of channels in cilia. *Cilia* **1**, 16.
Van Houten, J. (1998). Chemosensory transduction in *Paramecium*. *Eur. J. Protistol.* **34**, 301-307.
Wright, M. V. and Van Houten, J. L. (1990). Characterization of a putative Ca^{2+}-transporting Ca^{2+}-ATPase in the pellicles of *Paramecium tetraurelia*. *Biochim. Biophys. Acta* **1029**, 241-251.
Yano, J., Rachochy, V. and Van Houten, J. L. (2003). Glycosyl phosphatidylinositol-anchored proteins in chemosensory signaling: antisense manipulation of *Paramecium tetraurelia* PIG-A gene expression. *Eukaryot. Cell* **2**, 1211-1219.
Yano, J., Rajendran, A., Valentine, M. S., Saha, M., Ballif, B. A. and Van Houten, J. L. (2013). Proteomic analysis of the cilia membrane of *Paramecium tetraurelia*. *J. Proteomics* **78**, 113-122.